Focused Integration for Debris Observation (FIDO)

John E. Ploschnitznig
Modeling & Application Development Laboratory
Research & Engineering Group
Riverside Research

ABSTRACT

Satellites play a significant role in our day-to-day lives. They support communication, entertainment, travel, work, and many other areas that we now depend upon. However, as an increasing number of objects enter space and clutter this apparently endless vacuum, we find that these objects and their associated debris are becoming a potential and recurring threat. The space surveillance community routinely tracks and catalogs new entries into space, but debris from new systems and from failed existing systems are often missed and are becoming an increasing collision threat as more satellites are launched into space. The space surveillance community attempts to catalog debris through broad area search collection profiles, hoping to detect and track these elusive objects. Mechanical limitations of each collection system and how they are configured directly impacts the probability of detecting these very small objects. The United States Space Surveillance Network, consisting of very capable phase array systems, can scan massive volumes of space, yet many very small objects pass through undetected. Far too often, we are justly criticized for not "stepping out of the box" and the philosophy of "if it's not broke, don't fix it" works well only if you assume that it is not broken. The prevailing assumption that we need to increase our surveillance windows and cover as much space as possible to find new space debris might be appropriate if looking for large objects, but does not work well in trying to find small objects. Scanning large volumes of space increases the probability that objects will pass through the search beam, but it does not improve the ability to detect those objects. This paper proposes a paradigm shift which assumes that while large surveillance fences are necessary to see "many," we argue that a single focused beam may be critical to see "any." We refer to this concept as **F**ocused **I**ntegration for **D**ebris **O**bservation (FIDO), that is, "teaching an old dog new tricks."

1. DEBRIS

As humans began to inhabit space in Skylab, MIR, and most recently the International Space Station, safety became paramount. Air Force Space Command actively monitors all satellites and provides early notification for close-approach events through conjunction analysis. This monitoring while quite effective is not perfect, witness the Iridium collision with the Russian satellite on Feb 10, 2009. Although this event seriously impacted the Iridium mission, thankfully lives were not lost. For the crew of the ISS, such an event would have been devastating. Surprisingly, much smaller objects (on the order of only a few centimeters) could seriously damage the space station and could potentially result in loss of life. Manned space systems offer some protection, but only from small debris, several centimeters and smaller. Debris of this size is often very difficult to track, thus a method is needed which will allow NASA to detect much smaller debris than can currently be detected. We propose a concept, whimsically referred to as FIDO (**F**ocused **I**ntegration for **D**ebris **O**bservation), to fill this gap.

2. DEBRIS SIZE

Debris is usually of non-uniform shape, based on the definition of being a discarded part of something else. Our focus is not on naturally-occurring debris (space dust, asteroids, meteors, etc.), but rather on manmade artifacts from destroyed satellites, old rocket bodies, separation components, etc. The size of "small debris," in terms of its width/length dimensions, is on the order of centimeters. For a radar collection system with a nominal operating center frequency (f_c = 1GHz) and corresponding wavelength (λ), small centimeter-sized debris measures a fraction of a wavelength (less than 0.2λ). At these relative sizes, debris shape is no longer a determining factor in the scattering by such objects, which is determined by so-called Rayleigh scattering. In this scattering regime, the radar cross section (RCS) decreases dramatically as objects get smaller (i.e., RCS falls off as the fourth power of the wavelength). The particular version of the Raleigh scattering equation we employ in this paper is contained in the below figure (Fig. 1). Similar equations that differ slightly also exist, but display a similar trend and support the conclusions of our analysis.

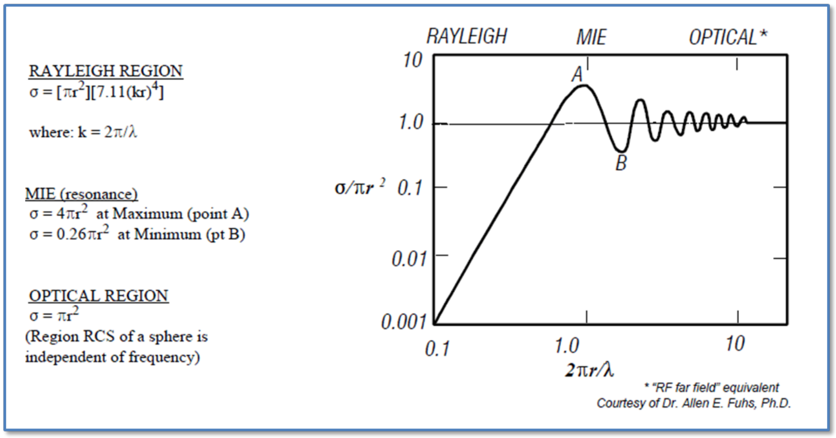

Fig. 1. RCS of a sphere [1]

3. DEBRIS LOCATION

Satellite location can be estimated by various means. We will rely on the use of the Space Command Simplified General Perturbation (SGP4) satellite propagation algorithm to display the location of the candidate debris. We also employ the Analytical Graphics Incorporated (AGI) Systems Tool Kit (STK) to propagate the notional debris and visualize the scenario (debris, radar, search volume, etc.) in 3-dimensional space. Various estimates exist of the number of objects in space; from tens of thousands to hundreds of thousands, depending on size considerations. "More than 21,000 orbital debris larger than 10 cm are known to exist. The estimated population of particles between 1 and 10 cm in diameter is approximately 500,000. The number of particles smaller than 1 cm exceeds 100 million" [2].

In this paper we consider debris between 300 - 600 kilometers in altitude. To gather a sample set, we queried the AGI Space Catalog for satellites in this altitude range that are primarily in circular orbits. Seventy-seven satellites were found and propagated, and the figure below (Fig. 2) shows the orbits of these satellites at a snapshot in time within a +/- 12 hour window, presented in an Earth Center Fixed (ECF) coordinate system. Since debris derives primarily from manmade objects, we assume that it will exist in similar orbits. For analysis purposes, we take these 77 satellites as our debris sample set. Our goal is to characterize where debris is most likely to transit through the Radar Field of Regard (FOR) to logically focus our radar resources.

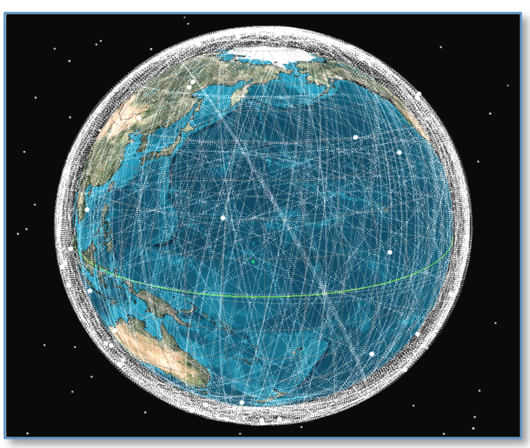

Fig. 2. 24-hour, 77 satellite track history

Fortunately, debris cannot change its orbital path without external intervention. As long as debris objects remain in the higher 300 to 600 km altitude, their trajectories can be modeled and characterized with routine collection updates. As the debris decays to lower altitudes, environmental factors impact its ability to maintain its orbit, with the result being that the debris will ultimately reenter the atmosphere. These factors become more of an issue as our characteristic debris descends towards 300 km.

4. RADAR

Our aim is to consider new ways to operate existing radars to find smaller debris, essentially "teaching an old dog new tricks." Radar systems are very similar and can be generalized using a notional radar range equation, despite system differences to support unique collection scenarios dictated by the specific mission (missile warning, space surveillance, aircraft surveillance, missile defense, tracking, etc.). The radar systems we will be simulating are used to support the United States Air Force Space Surveillance Network, and these consist of both large phased array radars and tracking dish radars. Generally, phased array radar systems offer very agile electronic beam steering which is very attractive in supporting large volume search operations. Dish radars have historically been paired with these large surveillance radars to track individual objects while the large search radars continue their surveillance mission. Discussing the pros and cons concerning specific capabilities of these various radar systems and missions can consume many hours, but the focus of this paper is to suggest a means of improving the detection of a single object in a single beam, rather than addressing the problem of finding many objects across many beams. Ultimately this becomes an academic discussion of radar resource management and overcoming the political argument of "more is better," and replacing it with the question, "Is it better to find many 10 cm targets versus any 4 cm targets?"

5. RADAR RESOURCE MANAGEMENT

Radar resource management effectively implements the radar range equation along with beam management to determine how much the radar can accomplish in a given period of time. Beam steering is a very important issue when discussing phase array radars since beams can be rapidly steered to any desired location within the radar field of regard, whereas a dish can only move sequentially in azimuth and elevation to adjacent beam locations as limited by the mechanical nature of the supporting pedestal. In both cases, pulses are generated for a specific location, at a specific rate (Pulse Repetition Frequency – PRF), and for a specific duration limited by the duty factor. Some of these parameters are driven by the physical limitations of the radar, while others are designed for the specific collection need. In this analysis, resource management equations will be utilized to demonstrate how a notional radar search profile can be configured to support typical surveillance missions and how it can be configured to support the debris discovery mission by employing our FIDO concept. Our focus is on relative trend analysis rather than absolute accuracy.

6. ANALYSIS

To properly analyze the data, we begin with known information. Since our analysis is notional, we work with a hypothetical (but realistic) satellite dataset (i.e., the previously mentioned 77 satellites serving as debris). The first step is to investigate the current space surveillance catalog and employ existing ephemeris data on all satellites to identify volumes of space with a high likelihood of encountering a transiting satellite. For this demonstration, a 24 hour scenario was conducted which propagated the 77 satellites. A random location (Kwajalein Island) was selected as a candidate from which to conduct the analysis. STK provided access information on all 77 satellites and a topographic coverage diagram (Fig. 3) which presents azimuth and elevation regions that can serve as candidate sensor locations for high probability of collection (line-of-sight access). From this information, it was quite evident that the highest probability of observing debris occurred at lower elevations (below 10 degrees) and at discrete azimuth locations. The black concentric annular rings represent contours of increasing elevation (with respect to the horizon) in 10 degree steps.

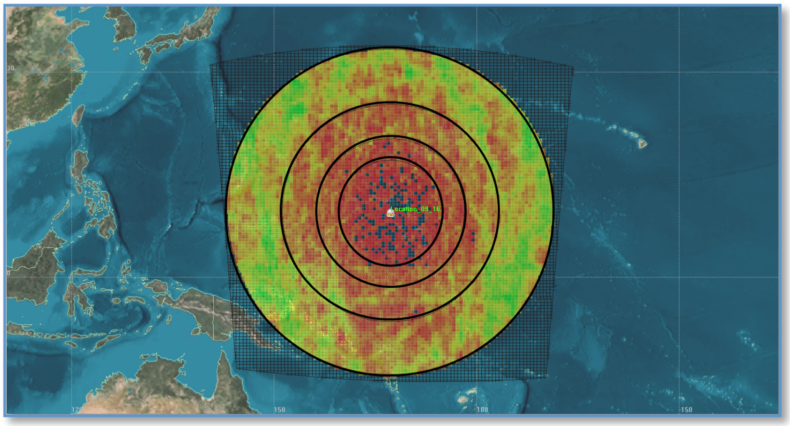

Fig. 3. Satellite azimuth and elevation coverage diagram

An azimuth versus elevation plot was generated from the access data (Fig. 4). This plot gathers data into 1 degree by 1 degree cells, ranging from -180 to +180 degrees in azimuth (0 is north, negative is West, positive is East) and 0 to 10 degrees in elevation (0 is horizon). Based on the data distribution in azimuth and elevation, it is apparent that a horizontal fence appears more likely to increase the likelihood of access.

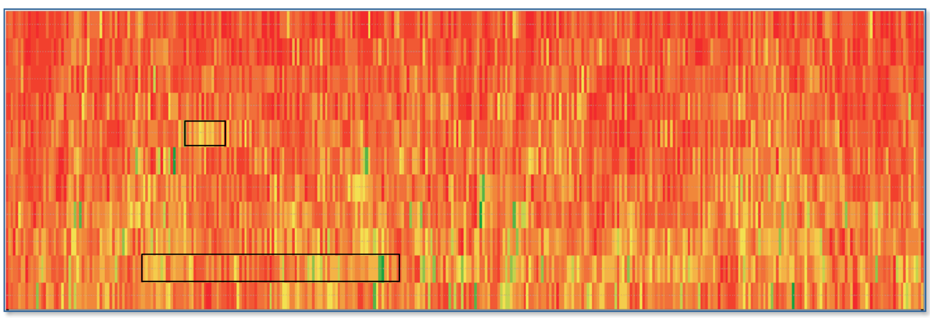

Fig. 4. 24-hour satellite azimuth versus elevation intercepts (0 to 10 degrees elevation)

A 10 degree search fan also appears to be a suitable width for the detection fan to cover a range of high access opportunities. A second filter was applied which averaged data over a +5 to -5 degree window in azimuth and 1 degree in elevation centered about a boresite vector (Fig. 5). This grid plots data from -180 to 180 degrees in azimuth and 0 to 10 degrees in elevation. This was used to select candidate detection fans in azimuth and elevation.

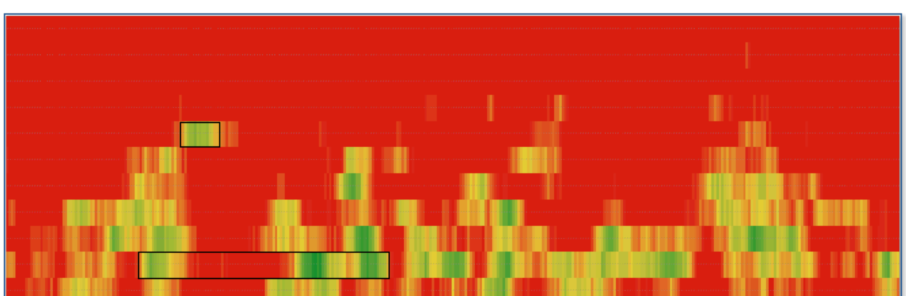

Fig. 5. 24-hour satellite 10 degree window w.r.t. azimuth and elevation (0 to 10 degrees elevation)

Surveillance radars are designed to detect and track satellites that are usually much larger than debris. A notional radar system will be configured to track satellites that break the horizon at the farthest range. The system will have a 1 degree beamwidth and scan over a 100 degree azimuth sector (surveillance mode), effectively defining 100 unique beam locations (assuming no overlap). The radar will scan from -27 to -127 in azimuth and 1 to 2 degrees in elevation (effectively 1 layer of 100 beams). To capture objects passing through from 300 to 600 km in altitude, the radar must be able to process objects from 1700 to 2700 km in range with respect to the radar. We set the notional settings to simulate a 1 GHz radar, with 6% duty factor, peak power of 10 Megawatts, and PRF of 50 Hz to satisfy the unambiguous range window. This effectively allows the radar to repeat its 100 degree scan every 2 seconds. Table 1 provides all of the relevant parameters for this notional radar.

Radar Physical Parameters

Freq	1	GHz
Beamwidth	1	deg
PEAK Power	10	MW
Duty Factor	6.00%	
Wavelength	0.299792458	m
Average Power	**0.6**	MW
Power	**57.7815125**	dBW
Gain	**46.15455129**	dBi
Effective Receive Aperture (Ar)	295.0439208	m^2
PowerAperture	**177.0263525**	Wm^2

Radar Operating Parameters

PRF	**50.00**	Hz
Duty Factor	**6.00%**	%
PRI (Pulse to Pulse time)	0.020000	sec
RCV Processing Time (necessary to distinguish Targets)	**1.200000**	msec
Pulse Length (Maximum travel distance of the beginning edge of the Pulse)	5995.85	km
"ON" Equivalent One-Way Distance	359.75	km
RCV Processing Equivalent One-Way Distance	359.75	km
Min Unambig Range	**179.88**	km
Max Unambig Range	**2818.05**	km
Max Data Collection Window (from min to max)	2638.17	km

SEARCH PARAMETERS

Volume 1		
Search Volume Height (Multiplier of beamwidth)	1.000	deg
Search Volume Width	100.000	deg
Solid Angle to be searched	100.000	deg^2
Total Volume		
Solid Angle to be searched	100.000	deg^2
Number of beams to search	**100.000**	beams

Missile Parameters

Satellite Fly-Through Rate	0.25	deg/s
Number of required hits per beam for Pd	1	
Revisit Time Requirement	**4.00**	sec
Dwell Time (time for Beam Position) - Effectively time for one PRI	0.020	sec
Revisit Time (Time to Scan Volumes)	**2.000**	sec
Pulses per second per beam location	0.500	sec
Pulses on target during the full transit	**2.000**	pulses
Time Left for additional Tasking	2.000	sec

Table 1. Generic radar parameters

Historically, such radars were requested to support debris search exercises on a yearly basis. Given these settings and an assumed target Signal to Noise threshold of 11 dB, a minimum RCS of -15 dBsm can be defined, which corresponds to a 20 cm diameter piece of debris (at 600 km altitude) that can be detected passing through the 100 degree search fan at max range. This is based on single pulse detection on a 20 cm diameter sphere (Physical Optics – PO approximation). This minimum detection level would not be adequate for debris detection over the full 100 degrees. Even with noncoherent integration of 2 pulses (max allowed for this 100 degree scan width notional radar with an estimated transiting debris angular rate of 0.25 degrees per second), we could only detect a -16 dBsm object (Table 2) which correlates to 18 cm diameter debris (using a general PO approximation).

Target RCS	-16
S/N	11

System (units)	Freq (GHz)	Ave Power (dBW)	Sys Temp (K)	Lt (dB)	Lr (dB)	La (dB)	Lp (dB)	Ls (dB)	Lw (dB)	Ld (dB)	Gain Tx (dB)	Gain Rcv (dB)	Integ N	Pulse (s)	RFLG @ 1ms (dB)	Range (km)
CASE 001	1.000	57.78	200.00	0.00	0.00	0.00	0.00	0.00	0.00	0.00	46.15	46.15	2.00	0.001200	283.75	**2745.46**

Table 2. CASE 001 radar performance

The final step in this analysis is to optimize this search fence to maximize detection performance. This requires us to define the unambiguous min and max range needed to cover the search volume, which extends from 300 km to 600 km in altitude. Also, selecting various PRF and duty factor settings will allow the operator to maximize the pulse length and keep energy on the transiting debris. Coherent and noncoherent integration may also be applied over successive pulses to lower noise, thus improving signal to noise values and allow detection of lower RCS debris.

For this example, we compare the 100 degree horizontal search fence to the 10 degree search fence and present the benefits of focusing collection on this dedicated area (Fig. 6). The 10 degree search fence spans from -98 to -108 in azimuth and 6 to 7 degrees in elevation. The higher elevation requires the search fence to extend from 1300 to 2200 km in range to monitor the 300 to 600 km debris altitude.

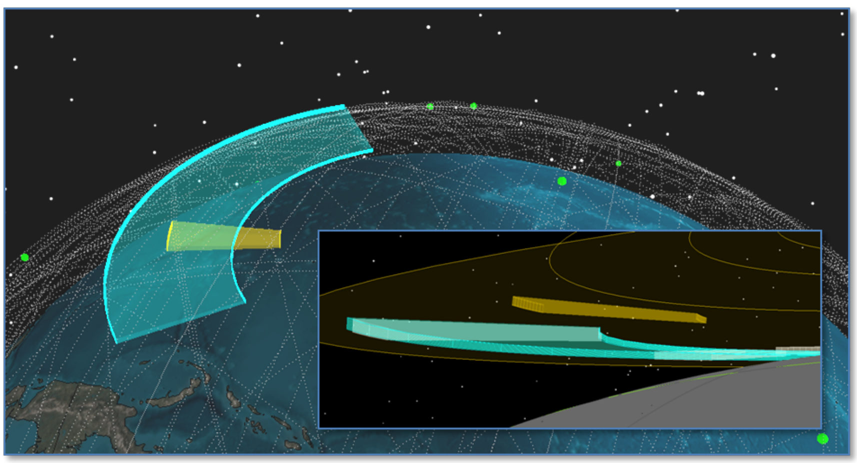

Fig. 6. Radar scan 100 degrees versus 10 degrees

During this phase, candidate radar systems are characterized to determine the necessary sensitivity levels to detect certain sized objects. Seven cases are defined with various parameter settings to explore ways for improving detection performance (Table 3). For example, PRF and Duty Factor directly affect the collection window and are adjusted to ensure an unambiguous search window in range.

Radar Physical Parameters	CASE 001	CASE 002	CASE 003	CASE 004	CASE 005	CASE 006	CASE 007	
Freq	1	1	1	1	1	1	1	GHz
Beamwidth	1	1	1	1	1	1	1	deg
PEAK Power	10	10	10	10	10	10	10	MW
Duty Factor	6.00%	6.00%	6.00%	12.00%	25.00%	12.00%	25.00%	
Wavelength	0.2998	0.2998	0.2998	0.2998	0.2998	0.2998	0.2998	m
Average Power	**0.6**	**0.6**	**0.6**	**1.2**	**2.5**	**1.2**	**2.5**	MW
Power	**57.7815**	**57.7815**	**57.7815**	**60.7918**	**63.9794**	**60.7918**	**63.9794**	dBW
Gain	**46.1546**	**46.1546**	**46.1546**	**46.1546**	**46.1546**	**46.1546**	**46.1546**	dBi
Effective Receive Aperture (Ar)	295.0439	295.0439	295.0439	295.0439	295.0439	295.0439	295.0439	m^2
PowerAperture	**177.0264**	**177.0264**	**177.0264**	**354.0527**	**737.6098**	**354.0527**	**737.6098**	Wm^2
Radar Operating Parameters								
PRF	**50.00**	**50.00**	**65.00**	**60.00**	**50.00**	**50.00**	**42.00**	Hz
Duty Factor	**6.00%**	**6.00%**	**6.00%**	**12.00%**	**25.00%**	**12.00%**	**25.00%**	%
PRI (Pulse to Pulse time)	0.020000	0.020000	0.015385	0.016667	0.020000	0.020000	0.023810	sec
RCV Processing Time (necessary to distinguish Targets)	**1.2000**	**1.2000**	**0.9231**	**2.0000**	**5.0000**	**2.4000**	**5.9524**	msec
Pulse Length (Maximum travel distance of the beginning edge of the Pulse)	5995.85	5995.85	4612.19	4996.54	5995.85	5995.85	7137.92	km
"ON" Equivalent One-Way Distance	359.75	359.75	276.73	599.58	1498.96	719.50	1784.48	km
RCV Processing Equivalent One-Way Distance	359.75	359.75	276.73	599.58	1498.96	719.50	1784.48	km
Min Unambig Range	**179.88**	**179.88**	**138.37**	**299.79**	**749.48**	**359.75**	**892.24**	km
Max Unambig Range	**2818.05**	**2818.05**	**2167.73**	**2198.48**	**2248.44**	**2638.17**	**2676.72**	km
Max Data Collection Window (from min to max)	2638.17	2638.17	2029.36	1898.69	1498.96	2278.42	1784.48	km
SEARCH PARAMETERS								
Volume 1								
Search Volume Height (Multiplier of beamwidth)	1.000	1.000	1.000	1.000	1.000	1.000	1.000	deg
Search Volume Width	100.000	10.000	10.000	10.000	10.000	100.000	100.000	deg
Solid Angle to be searched	100.000	10.000	10.000	10.000	10.000	100.000	100.000	deg^2
Total Volume								
Solid Angle to be searched	100.000	10.000	10.000	10.000	10.000	100.000	100.000	deg^2
Number of beams to search	**100.000**	**10.000**	**10.000**	**10.000**	**10.000**	**100.000**	**100.000**	beams
Missile Parameters								
Satellite Fly-Through Rate	0.25	0.25	0.25	0.25	0.25	0.25	0.25	deg/s
Number of required hits per beam for Pd	2	20	26	24	20	2	1	
Revisit Time Requirement	**2.00**	**0.20**	**0.15**	**0.17**	**0.20**	**2.00**	**4.00**	sec
Dwell Time (time for Beam Position) - Effectively time for one PRI	0.020	0.020	0.015	0.017	0.020	0.020	0.024	sec
Revisit Time (Time to Scan Volumes)	**2.000**	**0.200**	**0.154**	**0.167**	**0.200**	**2.000**	**2.381**	sec
Pulses per second per beam location	0.500	5.000	6.500	6.000	5.000	0.500	0.420	sec
Pulses on target during the full transit	**2.000**	**20.000**	**26.000**	**24.000**	**20.000**	**2.000**	**1.680**	pulses
Time Left for additional Tasking	0.000	0.000	0.000	0.000	0.000	0.000	1.619	sec

Table 3. CASE radar parameters

Physically scanning 10 degrees rather than 100 degrees immediately increases the available time dedicated to finding a potential target. This allows the mission planner to either increase the pulse length or the number of pulses on target (which offers the opportunity for additional integration). Tables 4 and 5 illustrate how the various settings can be adjusted to improve the likelihood of detecting smaller RCS targets, thus detecting smaller debris.

System	Freq (GHz)	Duty Factor	PRF (Hz)	Scan Width (deg)	Pulse (s)	Ave Power (dBW)	Sys Temp (K)	Losses (dB)	Gain Tx (dB)	Gain Rcv (dB)	Integ N	RFLG (dB)	S/N	Min Range (km)	Max Range (km)
CASE 001	1.000	6.00%	50.00	100	0.001200	57.78	200.00	0.00	46.15	46.15	2.00	284.54	11	1700	2700
CASE 002	1.000	6.00%	50.00	**10**	0.001200	57.78	200.00	0.00	46.15	46.15	**20.00**	**289.54**	11	**1300**	**2200**
CASE 003	1.000	6.00%	**65.00**	**10**	**0.000923**	57.78	200.00	0.00	46.15	46.15	**26.00**	**288.97**	11	**1300**	**2200**
CASE 004	1.000	**12.00%**	**60.00**	**10**	**0.002000**	**60.79**	200.00	0.00	46.15	46.15	**24.00**	**295.17**	11	**1300**	**2200**
CASE 005	1.000	**25.00%**	50.00	**10**	**0.005000**	**63.98**	200.00	0.00	46.15	46.15	**20.00**	**301.94**	11	**1300**	**2200**
CASE 006	1.000	**12.00%**	50.00	100	**0.002400**	**60.79**	200.00	0.00	46.15	46.15	2.00	**290.57**	11	1700	2700
CASE 007	1.000	**25.00%**	**42.00**	100	**0.005952**	**63.98**	200.00	0.00	46.15	46.15	**1.00**	**296.19**	11	1700	2700

Table 4. CASE radar settings and constraints

System	DEBRIS RCS -16	-17	-18	-19	-20	-21	-22	-23	-24	-25	-26	-27	-28	-29	-30	-31
CASE 001	2745	2592	2447	2310	2181	2059	1944	1835	1732	1635	1544	1458	1376	1299	1226	1158
CASE 002	3661	3456	3263	3080	2908	2745	2592	2447	2310	2181	2059	1944	1835	1732	1635	1544
CASE 003	3543	3345	3158	2981	2814	2657	2508	2368	2235	2110	1992	1881	1776	1676	1583	1494
CASE 004	5061	4778	4511	4258	4020	3795	3583	3382	3193	3015	2846	2687	2536	2395	2261	2134
CASE 005	7473	7055	6661	6288	5936	5604	5291	4995	4715	4452	4203	3967	3745	3536	3338	3151
CASE 006	3883	3665	3460	3267	3084	2912	2749	2595	2450	2313	2183	2061	1946	1837	1734	1637
CASE 007	5368	5068	4784	4517	4264	4025	3800	3588	3387	3198	3019	2850	2690	2540	2398	2264

System	-32	-33	-34	-35	-36	-37	-38	-39	-40	-41	-42	-43	-44	-45	-46	-47
CASE 001	1093	1032	974	920	868	820	774	730	690	651	615	580	548	517	488	461
CASE 002	1458	1376	1299	1226	1158	1093	1032	974	920	868	820	774	730	690	651	615
CASE 003	1410	1332	1257	1187	1120	1058	999	943	890	840	793	749	707	667	630	595
CASE 004	2015	1902	1796	1695	1600	1511	1426	1347	1271	1200	1133	1070	1010	953	900	850
CASE 005	2975	2809	2652	2503	2363	2231	2106	1988	1877	1772	1673	1579	1491	1408	1329	1255
CASE 006	1546	1459	1378	1301	1228	1159	1094	1033	975	921	869	821	775	731	690	652
CASE 007	2137	2017	1905	1798	1698	1603	1513	1428	1348	1273	1202	1135	1071	1011	955	901

Table 5. CASE RCS performance chart

CASE 001 is the reference case for a 100 degree horizon sensor which searches for debris from 1700 to 2700 km in range. Table 5 extends this table by illustrating in three-colors where the RCS (column headings range from debris RCS of -16 to -47 dBsm) can be detected in one of three locations:

1. GREEN – Greater than MAX Range
2. YELLOW – Greater than MIN Range and Less than MAX Range
3. RED – Less than MIN Range

Focusing on the transition from green to yellow defines the lowest RCS debris that can be detected at 600 km in altitude, and the transition from yellow to red indicates the lowest RCS debris that can be detected at 300 km. These variables are not mutually exclusive. Explaining how the variables are connected and dependent on each other is beyond the scope of this paper, but the key finding from this exercise is that there are several ways to improve detection performance once reducing the search window is considered. This leads to immediate radar resource savings and allows the operator to manage other parameters (PRF, Duty Factor, Integration, etc.) to improve the probability of detection in the new search area.

Since our focus is on small objects, we wish to detect objects -25 dBsm and lower (ref. Table 6). For 1 GHz radar, an RCS of -25 dBsm falls in the upper end of the Rayleigh scattering regime and corresponds to a physical object approximately 6 cm in diameter (comparable to a lacrosse ball). No case can detect objects below -47 dBsm which corresponds to a ping pong ball sized object. For RCS values greater than -25 dBsm, we usually enter the Mie resonance scattering regime. Since debris is not spherical, the associated resonance behavior corresponding to the observed constructive and destructive interference pattern and attributed to creeping wave effects is not present. For performance comparisons, larger RCS objects can be calculated using Physical Optics calculations.

Tables 4 and 5 present radar settings (CASEs) and the corresponding RCS performance (detectable debris RCS levels). To illustrate the benefit of FIDO, we examine two cases in detail. CASE 001, corresponding to notional radar settings for a 100 degree surveillance fence, allows the radar to detect -16 dBsm (Table 5 column header) debris at 2745 km, which is beyond the max range of the detection window. This entry in Table 5 is GREEN since debris at this RCS level can be detected anywhere within the radar unambiguous surveillance range window (1700 to 2700 km). Debris at -25 dBsm can only be detected at 1635 km or less, falling short of the range window lower limit of 1700 km in this case. Since it cannot be detected anywhere within the range window it is RED. Debris in the range from -17 to -24 dBsm can be detected at various ranges within the range window, with the larger -17 dBsm debris detectable close to the max range, and the smaller -24 dBsm debris detectable close to the minimum range window extent. These are all YELLOW since they can be detected within the CASE 001 radar unambiguous surveillance range window, but not over the full range window (1700 to 2700 km).

We now compare CASE 001 (100 degree search fence) to CASE 002 through 005 that have a 10 degree search fence. CASE 002 is most similar to CASE 001, but with a 10 degree search fence, and its higher elevation pointing reduces the search window range extent (1300 to 2200 km). Just these two changes alone improve detection performance by approximately 8 dB. The previous CASE 001 minimum detectable RCS (-24 dBsm) at min range is now detectable across the entire CASE 002 radar unambiguous surveillance range window. This is primarily due to the increased number of pulses available for noncoherent integration. CASE 002 offers a minimum detectable RCS of -33 dBsm at 1376 km (just within the range window). CASE 004 and 005 extend the radar performance by increasing the duty factor and PRF. Similar techniques can be applied to the CASE 001 configuration (cf. CASE 005 and CASE 006), but nothing can account for the resources gained by simply reducing the 100 degree search fence to the focused 10 degree search fence.

Rayleigh Scattering

Speed of light	m/s	299,792,458.00
		X-band
Frequency	Ghz	1.000
Bandwidth	Ghz	0.10
Weighting Factor		0.00
Wavelength	m	0.2998
Radius Step Size		0.00050

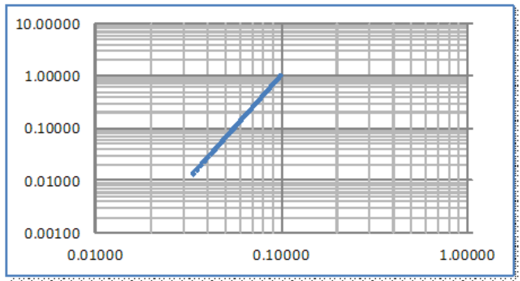

		Radius	Radius/Lamda Percentage	Raleigh σ Arith	Raleigh σ Geom	Horiz Arith	Vert Arith
Radius of the Sphere	m	0.01000	0.033356	4.30979E-06	-53.66	0.03336	0.01372
		0.01050	0.035024	5.77553E-06	-52.38	0.03502	0.01667
		0.01100	0.036692	7.63506E-06	-51.17	0.03669	0.02009
		0.01150	0.038360	9.96881E-06	-50.01	0.03836	0.02399
		0.01200	0.040028	1.2869E-05	-48.90	0.04003	0.02845
Ping-Pong Ball		0.01250	0.041696	1.64405E-05	-47.84	0.04170	0.03349
		0.01300	0.043363	2.08025E-05	-46.82	0.04336	0.03918
		0.01350	0.045031	2.60891E-05	-45.84	0.04503	0.04557
		0.01400	0.046699	3.24507E-05	-44.89	0.04670	0.05270
		0.01450	0.048367	4.00557E-05	-43.97	0.04837	0.06064
		0.01500	0.050035	4.90912E-05	-43.09	0.05003	0.06945
		0.01550	0.051702	5.97649E-05	-42.24	0.05170	0.07918
		0.01600	0.053370	7.23063E-05	-41.41	0.05337	0.08991
		0.01650	0.055038	8.69681E-05	-40.61	0.05504	0.10168
		0.01700	0.056706	0.000104028	-39.83	0.05671	0.11458
		0.01750	0.058374	0.00012379	-39.07	0.05837	0.12866
		0.01800	0.060042	0.000146586	-38.34	0.06004	0.14401
		0.01850	0.061709	0.000172777	-37.63	0.06171	0.16069
		0.01900	0.063377	0.000202758	-36.93	0.06338	0.17878
		0.01950	0.065045	0.000236954	-36.25	0.06504	0.19836
		0.02000	0.066713	0.000275827	-35.59	0.06671	0.21950
		0.02050	0.068381	0.000319874	-34.95	0.06838	0.24228
		0.02100	0.070048	0.000369634	-34.32	0.07005	0.26680
		0.02150	0.071716	0.000425684	-33.71	0.07172	0.29313
		0.02200	0.073384	0.000488644	-33.11	0.07338	0.32136
		0.02250	0.075052	0.00055918	-32.52	0.07505	0.35159
		0.02300	0.076720	0.000638004	-31.95	0.07672	0.38390
		0.02350	0.078388	0.000725877	-31.39	0.07839	0.41839
		0.02400	0.080055	0.000823614	-30.84	0.08006	0.45515
		0.02450	0.081723	0.000932079	-30.31	0.08172	0.49428
		0.02500	0.083391	0.001052195	-29.78	0.08339	0.53588
		0.02550	0.085059	0.001184942	-29.26	0.08506	0.58005
		0.02600	0.086727	0.001331362	-28.76	0.08673	0.62690
		0.02650	0.088394	0.001492559	-28.26	0.08839	0.67653
		0.02700	0.090062	0.001669701	-27.77	0.09006	0.72906
		0.02750	0.091730	0.001864027	-27.30	0.09173	0.78458
		0.02800	0.093398	0.002076846	-26.83	0.09340	0.84322
		0.02850	0.095066	0.002309539	-26.36	0.09507	0.90508
		0.02900	0.096734	0.002563564	-25.91	0.09673	0.97028
Lacrosse Ball		0.02950	0.098401	0.002840457	-25.47	0.09840	1.03895

Table 6: Rayleigh Scattering RCS

7. CONCLUSIONS

Based on our analysis, we conclude that the FIDO concept of employing narrower search windows for the purpose of detecting smaller (i.e., lower RCS) debris is superior to the conventional method of using large search windows, that is based on the erroneous assumption that more objects will be captured. The fallacy of the latter approach is that while it is true that more objects will transit through the larger search window, the radar will lack the sensitivity to detect and track the smaller debris.

FIDO intends to bring awareness to the logical available options for helping to detect smaller objects. Changing the mindset of the in-the-box thinker can be as difficult as actually designing an optimized search fence. If successful, FIDO should expand the capabilities of legacy radars to be effective for a whole new regime of important targets, namely, problematic small debris objects.

8. ACKNOWLEDGEMENT

We would like to thank Analytical Graphics Incorporated for the use of Systems Tool Kit (STK) to perform this analysis. STK offers a simple user interface to load and propagate many satellites, collection systems, and search fences to visually convey complex data in a realistic visualization environment.

9. REFERENCES

1. Fuhs, A. E., Radar Cross Section Lectures, Naval Postgraduate School, DTIC File Copy, 1983.
2. NASA Orbital Debris Program Office (Last Updated March 2012), Orbital Debris FAQ, Retrieved August 2013, from http://orbitaldebris.jsc.nasa.gov/faqs.html#3.